J|A|C|S
ARTICLES
Published on Web 12/27/2001

Infrared Spectra of $C_3H_3^+$-N_2 Dimers: Identification of Proton-Bound c-$C_3H_3^+$-N_2 and H_2CCCH^+-N_2 Isomers

Otto Dopfer,* Doris Roth, and John P. Maier

Contribution from the Institute for Physical Chemistry, University of Basel, Klingelbergstrasse 80, CH-4056 Basel, Switzerland

Received August 20, 2001

Abstract: Mid-infrared photodissociation spectra of mass selected $C_3H_3^+$-N_2 ionic complexes are obtained in the vicinity of the C−H stretch fundamentals (2970−3370 cm^{-1}). The $C_3H_3^+$-N_2 dimers are produced in an electron impact cluster ion source by supersonically expanding a gas mixture of allene, N_2, and Ar. Rovibrational analysis of the spectra demonstrates that (at least) two $C_3H_3^+$ isomers are produced in the employed ion source, namely the cyclopropenyl (c-$C_3H_3^+$) and the propargyl (H_2CCCH^+) cations. This observation is the first spectroscopic detection of the important c-$C_3H_3^+$ ion in the gas phase. Both $C_3H_3^+$ cations form intermolecular proton bonds to the N_2 ligand with a linear −C−H···N−N configuration, leading to planar $C_3H_3^+$-N_2 structures with C_{2v} symmetry. The strongest absorption of the H_2CCCH^+-N_2 dimer in the spectral range investigated corresponds to the acetylenic C−H stretch fundamental ($\nu_1 = 3139$ cm^{-1}), which experiences a large red shift upon N_2 complexation ($\Delta\nu_1 \approx -180$ cm^{-1}). For c-$C_3H_3^+$-N_2, the strongly IR active degenerate antisymmetric stretch vibration (ν_4) of c-$C_3H_3^+$ is split into two components upon complexation with N_2: $\nu_4(a_1) = 3094$ cm^{-1} and $\nu_4(b_2) = 3129$ cm^{-1}. These values bracket the yet unknown ν_4 frequency of free c-$C_3H_3^+$ in the gas phase, which is estimated as 3125 ± 4 cm^{-1} by comparison with theoretical data. Analysis of the nuclear spin statistical weights and *A* rotational constants of H_2CCCH^+-N_2 and c-$C_3H_3^+$-N_2 provide for the first time high-resolution spectroscopic evidence that H_2CCCH^+ and c-$C_3H_3^+$ are planar ions with C_{2v} and D_{3h} symmetry, respectively. Ab initio calculations at the MP2(full)/6-311G(2df,2pd) level confirm the given assignments and predict intermolecular separations of $R_e = 2.1772$ and 2.0916 Å and binding energies of $D_e = 1227$ and 1373 cm^{-1} for the H-bound c-$C_3H_3^+$-N_2 and H_2CCCH^+-N_2 dimers, respectively.

I. Introduction

The $C_3H_3^+$ ion is a fundamental hydrocarbon cation and plays a central role for many important processes in physical and organic chemistry. Two isomeric structures of $C_3H_3^+$ have previously been identified by mass spectrometric and spectroscopic techniques[1−10] and both are also observed in the present work (Figure 1): the cyclic planar cyclopropenyl cation (c-$C_3H_3^+$, D_{3h}) and the open-chain planar propargyl cation (H_2CCCH^+, C_{2v}). c-$C_3H_3^+$ is the smallest aromatic cation with two delocalized π electrons and is ≈25 kcal/mol more stable than H_2CCCH^+.[2] This experimental observation is confirmed by numerous ab initio calculations, which predict high barriers to interconversion between the two most stable $C_3H_3^+$ isomers.[11−15] Other $C_3H_3^+$ isomers (e.g., CH_3CC^+ and H_2CCHC^+) are calculated to be significantly less stable than c-$C_3H_3^+$ and H_2CCCH^+ and have not been identified experimentally.[12−15] Both H_2CCCH^+ and c-$C_3H_3^+$ are considered to be central

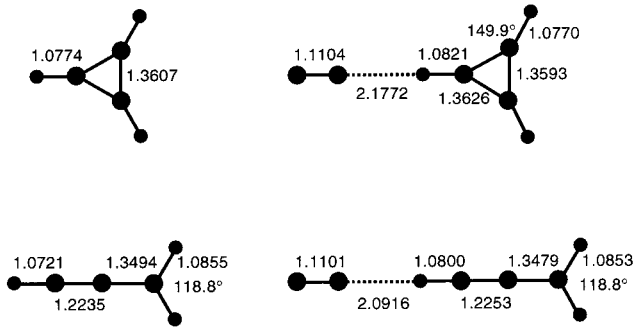

Figure 1. Geometrical data (in Å) of the minimum structures of c-$C_3H_3^+$, H_2CCCH^+, and their complexes with N_2 calculated at the MP2(full)/6-311G(2df,2pd) level. The interatomic separation in free N_2 is calculated as 1.1108 Å.

* Corresponding author: e-mail otto.dopfer@unibas.ch; phone ++41 61 267 3823; fax ++41 61 267 3855.

(1) Breslow, R.; Groves, J. T. *J. Am. Chem. Soc.* **1970**, *92*, 984.
(2) Lossing, F. P. *Can. J. Chem.* **1972**, *50*, 3973.
(3) Ausloos, P. J.; Lias, S. G. *J. Am. Chem. Soc.* **1981**, *103*, 6505.
(4) Craig, N. C.; Pranata, J.; Reinganum, S. J.; Sprague, J. R.; Stevens, P. S. *J. Am. Chem. Soc.* **1986**, *108*, 4378.
(5) Minsek, D. W.; Chen, P. *J. Phys. Chem.* **1990**, *94*, 8399.
(6) McEvan, M. J.; McConnell, C. L.; Freeman, C. G.; Anicich, V. G. *J. Phys. Chem.* **1994**, *98*, 5068.
(7) Scott, G. B. I.; Fairley, D. A.; Freeman, C. G.; McEvan, M. J.; Anicich, V. G. *J. Phys. Chem. A* **1999**, *103*, 1073.
(8) Scott, G. B. I.; Milligan, D. B.; Fairly, D. A.; Freeman, C. G.; McEvan, M. J. *J. Chem. Phys.* **2000**, *112*, 4959.
(9) Gilbert, T.; Pfab, R.; Fischer, I.; Chen, P. *J. Chem. Phys.* **2000**, *112*, 2575.
(10) Wyss, M.; Riaplov, E.; Maier, J. P. *J. Chem. Phys.* **2001**, *114*, 10355.
(11) Raghavachari, K.; Whiteside, R. A.; Pople, J. A.; Schleyer, P. v. R. *J. Am. Chem. Soc.* **1981**, *103*, 5649.
(12) Hopkinson, A. C.; Lien, M. H. *J. Am. Chem. Soc.* **1986**, *108*, 2843.
(13) Wong, M. W.; Radom, L. *J. Am. Chem. Soc.* **1989**, *111*, 6976.
(14) Cameron, A.; Leszczynski, J.; Zerner, M. C.; Weiner, B. *J. Phys. Chem.* **1989**, *93*, 139.
(15) Maluendes, S. A.; McLean, A. D.; Yamashita, K.; Herbst, E. *J. Chem. Phys.* **1993**, *99*, 2812.

10.1021/ja012004p CCC: $22.00

Table 1. Harmonic Frequencies (unscaled), Complexation-Induced Frequency Shifts (in cm^{-1}), IR Intensities (in km/mol) and Symmetry Species for the Vibrations of c-$C_3H_3^+$ (D_{3h}), H_2CCCH^+ (C_{2v}), and their H-Bound N_2 Complexes (C_{2v}) Calculated at the MP2(full)/6-311G(2df,2pd) Level (For Comparison, Available Experimental Fundamental Frequencies Are Listed)

mode	H_2CCCH^+/N_2 exp[a]	H_2CCCH^+/N_2 calc	H_2CCCH^+-N_2 calc	Δ calc	mode	c–$C_3H_3^+/N_2$ exp[b]	c-$C_3H_3^+/N_2$ calc	c-$C_3H_3^+$-N_2 calc	Δ calc
$\nu_1(a_1)$	3319	3412 (113)	3297 (486)	−115	ν_1	3183	3352 (0/a_1')	3344 (2/a_1)	−8
$\nu_2(a_1)$	3130	3155 (22)	3156 (18)	1	ν_2	1626	1657 (0/a_1')	1653 (3/a_1)	−4
$\nu_3(a_1)$	2122	2257 (395)	2239 (617)	−18	ν_3	(1031)	1057 (0/a_2')	1075 (0/b_1)	18
$\nu_4(a_1)$	1465	1499 (9)	1500 (12)	1	ν_4	3138	3302 (225/e′)	3243 (364/a_1)	−59
$\nu_5(a_1)$	(1106)	1141 (29)	1144 (11)	3				3305 (105/b_2)	3
$\nu_6(b_1)$	1183	1160 (9)	1156 (9)	−4	ν_5	1290	1339 (77/e′)	1340 (63/a_1)	1
$\nu_7(b_1)$	(910)	881 (8)	974 (5)	93				1333 (36/b_2)	−6
$\nu_8(b_1)$		273 (25)	301 (20)	28	ν_6	927	953 (64/e′)	952 (25/a_1)	−1
$\nu_9(b_2)$		3266 (47)	3268 (43)	2				982 (23/b_2)	29
$\nu_{10}(b_2)$		1049 (1)	1050 (1)	1	ν_7	758	784 (70/a_2'')	806 (61/b_1)	22
$\nu_{11}(b_2)$		696 (43)	815 (31)	119	ν_8	(990)	1032 (0/e″)	1032 (0/a_2)	0
$\nu_{12}(b_2)$		294 (21)	306 (16)	12				1079 (1/b_2)	47
ν_s (a_1)			120 (26)		ν_s			108 (22/a_1)	
$\nu_b(b_1)$			118 (0)		ν_b			126 (0/b_1)	
$\nu_b(b_1)$			51 (0)		ν_b			68 (0/b_1)	
$\nu_b(b_2)$			123 (0)		ν_b			112 (1/b_2)	
$\nu_b(b_2)$			53 (0)		ν_b			55 (0/b_2)	
ν_{N-N}	2330[c]	2204 (0)	2211 (7)	7	ν_{N-N}	2330[c]	2204 (0)	2208 (6)	4

[a] Gas-phase fundamental frequencies of H_2CCCH^+ are derived from ZEKE spectra of H_2CCCH with an uncertainty of ±10 cm^{-1} (ref 9). Values in parentheses are obtained from combination bands. [b] Fundamental frequencies of c-$C_3H_3^+$ are measured in liquid SO_2 or in polycrystalline c-$C_3H_3^+X^-$ salts (ref 4). Values in parentheses are derived from a normal coordinate analysis. [c] Gas-phase fundamental frequency (ref 64).

cations in the ion−molecule reaction chemistry of terrestrial and extraterrestrial hydrocarbon plasmas.[16−23] For example, c-$C_3H_3^+$ is assumed to be the major precursor for c-C_3H_2, an ubiquitous molecule in interstellar media.[20−24] Similarly, H_2CCCH^+ is likely to be involved in the production of interstellar H_2CCC.[21,25] The probable detection of c-$C_3H_3^+$ in the coma of comet Halley by mass spectrometry has also been reported.[26] In addition, c-$C_3H_3^+$ is a major ion in hydrocarbon flames and thus discussed as an important nucleation center for soot formation in combustion processes.[16−19] $C_3H_3^+$ is also a common fragment ion observed in the mass spectra of hydrocarbon molecules.

Despite their importance, spectroscopic information at the level of rotational resolution is lacking for all $C_3H_3^+$ isomers. Lower resolution studies of H_2CCCH^+ include photoelectron spectra,[5,9] yielding the fundamental frequencies for $\nu_1-\nu_7$ (Table 1), and a recent Ne matrix isolation spectrum.[10] No gas-phase spectrum is available for c-$C_3H_3^+$. However, nearly all fundamental frequencies of this ion are known from infrared (IR) spectra of polycrystalline c-$C_3H_3^+X^-$ salts,[1,4] Raman studies of such salts in liquid SO_2,[4] and an IR spectrum of c-$C_3H_3^+$ embedded in a Ne matrix.[10] Furthermore, ab initio data on the equilibrium structure, harmonic frequencies, and rotation−vibration parameters derived from anharmonic force fields are available for both c-$C_3H_3^+$ (refs 14 and 27−29) and H_2CCCH^+.[30,31]

The present work reports IR spectra and quantum chemical calculations of isomeric $C_3H_3^+$-N_2 dimers. The results provide new information about the structural, spectroscopic, and energetic properties of c-$C_3H_3^+$ and H_2CCCH^+ and their intermolecular interaction with N_2. Several weakly bound complexes of the type $C_3H_3^+$-X with stable molecules X have been identified in mass spectrometric studies.[6−8,32] Some of them correspond to collisionally stabilized intermediates of chemical reactions involving $C_3H_3^+$ and X. Often, the different reactivity of c-$C_3H_3^+$ and H_2CCCH^+ toward neutral molecules X is used to distinguish between both isomers (with H_2CCCH^+ being usually more reactive).[3,6−8] Selected ion flow tube studies show that both c-$C_3H_3^+$ and H_2CCCH^+ do not react with inert N_2.[7] In contrast to mass spectrometric studies, no spectroscopic data exist for $C_3H_3^+$-X dimers. Thus, the present study on $C_3H_3^+$-N_2 provides the first spectroscopic information about structure and stability of such complexes. Information about the intermolecular potential of $C_3H_3^+$-X dimers is desired to improve our understanding of the intermolecular interaction and ion−molecule reaction chemistry of the various $C_3H_3^+$ isomers. Interestingly, both $C_3H_3^+$ ions observed offer several favorable competing ligand binding sites. For example, in c-$C_3H_3^+$-N_2 the N_2 ligand may bind to the π-electron system of the aromatic ring (π-bond) or to one of the three equivalent carbon (C-bond) or hydrogen atoms (H-bond). IR spectra of benzene$^+$-N_2 and phenol$^+$-N_2 indicate that N_2 forms a π-bond to the benzene cation[33] and a H-bond to the O−H group of phenol$^+$.[34,35] In the case of H_2CCCH^+, N_2 may form a H-bond to a proton of

(16) Goodings, J. M.; Bohme, D. K.; Ng, C.-W. *Combust. Flame* **1979**, *36*, 27.
(17) Hayhurst, A. N.; Jones, H. R. N. *Nature* **1982**, *296*, 61.
(18) Graham, S. M.; Goodings, J. M. *Int. J. Mass Spectrosc. Ion Proc.* **1984**, *56*, 205.
(19) Hall-Roberts, V. J.; Hayhurst, A. N.; Knight, D. E.; Taylor, S. G. *Combust. Flame* **2000**, *120*, 578.
(20) Herbst, E.; Adams, N. G.; Smith, D. *Astrophys. J.* **1983**, *269*, 329.
(21) Adams, N. G.; Smith, D. *Astrophys. J.* **1987**, *317*, L25.
(22) Gerlich, D.; Horning, S. *Chem. Rev.* **1992**, *92*, 1509.
(23) Smith, D. *Chem. Rev.* **1992**, *92*, 1473.
(24) Thaddeus, P.; Vritilek, J. M.; Gottlieb, C. A. *Astrophys. J.* **1985**, *299*, L63.
(25) Cernicharo, J.; Gottlieb, C. A.; Guelin, M.; Killian, T. C.; Paubert, G.; Thaddeus, P.; Vrtilek, J. M. *Astrophys. J.* **1991**, *368*, L39.
(26) Korth, A.; Marconi, M. L.; Mendis, D. A.; Krueger, F. R.; Richter, A. K.; Lin, R. P.; Mitchell, D. L.; Anderson, K. A.; Carlson, C. W.; Reme, H.; Sauvaud, J. A.; d'Uston, C. *Nature* **1989**, *337*, 53.
(27) Xie, Y.; Boggs, J. E. *J. Chem. Phys.* **1989**, *90*, 4320.
(28) Lee, T. J.; Willetts, A.; Gaw, J. F.; Handy, N. C. *J. Chem. Phys.* **1989**, *90*, 4330.
(29) Galembeck, S. E.; Fausto, R. *J. Mol. Struct. (THEOCHEM)* **1995**, *332*, 105.
(30) Botschwina, P.; Horn, M.; Flügge, J.; Seeger, S. *J. Chem. Soc., Faraday Trans.* **1993**, *89*, 2219.
(31) Botschwina, P.; Oswald, R.; Flügge, J.; Horn, M. *Z. Phys. Chem.* **1995**, *188*, 29.
(32) Anicich, V. G. *J. Chem. Phys. Ref. Data* **1993**, *22*, 1469.
(33) Dopfer, O.; Olkhov, R. V.; Maier, J. P. *J. Chem. Phys.* **1999**, *111*, 10754.
(34) Solcà, N.; Dopfer, O. *Chem. Phys. Lett.* **2000**, *325*, 354.
(35) Solcà, N.; Dopfer, O. *J. Phys. Chem. A* **2001**, *105*, 5637.

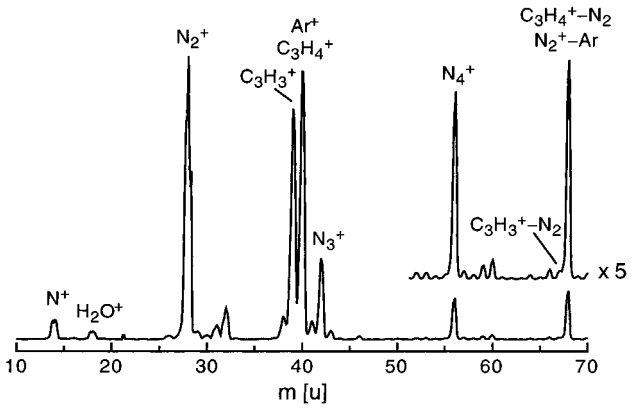

Figure 2. Typical mass spectrum of the ion source in the range 10−70 u obtained by expanding a gas mixture of allene (H_2CCCH_2), Ar, and N_2 in the ratio of 1:100:100 at a backing pressure of 5 bar. The spectrum is dominated by N_n^+, $Ar^+/C_3H_4^+$, N_2^+-Ar, and $C_3H_3^+$. The N_2^+ and Ar^+ peaks are saturated. The inset shows part of the mass spectrum expanded by a factor of 5 to show the mass peak of $C_3H_3^+$-N_2. The intensity ratio of the $C_3H_3^+$-N_2 and $C_3H_3^+$ peaks is of the order of 1:300.

either the CH_2 group or the acetylenic C−H bond. The IR spectra of $C_3H_3^+$-N_2 produced in a low-temperature supersonic plasma and the quantum chemical calculations presented in the present work will reveal the most favorable binding site of N_2 for both $C_3H_3^+$ isomers. Moreover, important spectral information about the properties of free c-$C_3H_3^+$ and H_2CCCH^+ can be derived from the rovibrational analysis of the $C_3H_3^+$-N_2 dimer spectra in conjunction with the calculations. This strategy is frequently called messenger technique and has been successfully employed to derive spectroscopic parameters of bare ions from their corresponding cluster spectra.[33,36−41]

II. Experimental Section

IR photodissociation spectra of $C_3H_3^+$-N_2 ionic complexes are recorded in a tandem mass spectrometer.[42,43] The complexes are produced in an ion source combining a pulsed and skimmed supersonic expansion with electron impact ionization.[42] All spectra shown in the present work are obtained by expanding a gas mixture of allene (H_2CCCH_2), Ar, and N_2 in the ratio of 1:100:100 at a backing pressure of 5 bar through a pulsed nozzle into a vacuum chamber. Electron impact ionization close to the nozzle orifice and subsequent ion−molecule and three-body association reactions lead to the formation of $C_3H_3^+$-N_2 complexes. A typical mass spectrum of the ion source in the range 10−70 u is reproduced in Figure 2. This mass spectrum is dominated by N_n^+, $Ar^+/C_3H_4^+$, N_2^+-$Ar/C_3H_4^+$-N_2, and $C_3H_3^+$. In agreement with previous electron impact mass spectra of allene, the by far largest fragment ion produced is the $C_3H_3^+$ ion.[44] The intensity ratio of the $C_3H_3^+$-N_2 and $C_3H_3^+$ mass peaks is of the order of 1:300. The IR spectrum of $C_3H_3^+$-N_2 complexes under these experimental conditions reveals high abundance of both H_2CCCH^+ and c-$C_3H_3^+$ in the ion source. To substantially suppress the production of one of the two isomers, allene has been replaced by other precursors. IR spectra recorded with propyne (H_3CCCH), 3-chloro-1-propyne (ClH_2CCCH), or benzene (C_6H_6) are, however, qualitatively similar to those obtained with allene, implying that the relative abundance of H_2CCCH^+ and c-$C_3H_3^+$ is roughly independent within this group of precursors. All spectra presented here are obtained employing allene because this precursor produces the by far largest $C_3H_3^+$-N_2 currents.

The produced ions are extracted from the source through a skimmer into a quadrupole mass spectrometer tuned to the mass of $C_3H_3^+$-N_2 (67 u). The mass selected dimer beam is then injected into an octopole ion guide, where it interacts with the counter propagating IR laser pulse. Photoexcitation of $C_3H_3^+$-N_2 into metastable rovibrational levels above the lowest dissociation threshold causes fragmentation into $C_3H_3^+$ and N_2. No other fragment channels are observed. The produced $C_3H_3^+$ fragment ions are selected by a second quadrupole mass filter (tuned to 39 u) and monitored as a function of the laser frequency to obtain the IR action spectrum of $C_3H_3^+$-N_2. Pulsed and tunable IR laser radiation is generated by an optical parametric oscillator (OPO) laser system pumped by a Nd:YAG laser. The laser frequency is calibrated to better than 0.02 cm^{-1} by optoacoustic reference spectra of HDO recorded simultaneously with the photodissociation spectrum using the signal output of the OPO, and interpolation between reference lines is facilitated by transmission étalon markers of the OPO oscillator. All line positions are corrected for the Doppler shift (+0.04 cm^{-1}) induced by the kinetic energy of the ions in the octopole ($E_{kin} = 6.5 \pm 0.5$ eV). The Doppler width derived from the estimated uncertainty in E_{kin} (0.002 cm^{-1}) is well below the laser bandwidth (0.02 cm^{-1}). All spectra are normalized for laser intensity variations by using an InSb IR detector.

III. Ab Initio Calculations

The electronic ground states of the closed-shell c-$C_3H_3^+$ and H_2CCCH^+ ions and their dimers with N_2 are investigated by ab initio and density functional calculations.[45] All results reported in the present work are obtained at the MP2(full)/6-311G(2df,2pd) level of theory. Extensive calculations have also been performed at the B3LYP level with the 6-311G(2df,2pd) basis set, as well as the HF, B3LYP, and MP2(full) levels with the 6-31G* basis set. The results of these lower level calculations are in qualitative agreement with the data obtained at the MP2(full)/6-311G(2df,2pd) level and are not discussed in detail further. The calculations provide information about structure and vibrational frequencies and IR intensities of the $C_3H_3^+$ isomers and their N_2 complexes. Moreover, the properties of the intermolecular interaction and its influence on the monomer ions are characterized (e.g., intermolecular separation and binding energy, intermolecular frequencies, effects of complexation on the monomer properties). The global minima on the respective intermolecular potentials are located by gradient optimization relaxing all coordinates, and the nature of stationary points is verified by frequency analysis. Calculated intermolecular binding energies of the dimers are fully counterpoise corrected for the basis set superposition error.[46] The results of the calculations are summarized in Figure 1 and Table 1. As the $C_3H_3^+$ normal modes

(36) Yeh, L. I.; Okumura, M.; Myers, J. D.; Price, J. M.; Lee, Y. T. *J. Chem. Phys.* **1989**, *91*, 7319.
(37) Nizkorodov, S. A.; Roth, D.; Olkhov, R. V.; Maier, J. P.; Dopfer, O. *Chem. Phys. Lett.* **1997**, *278*, 26.
(38) Bieske, E. J.; Dopfer, O. *Chem. Rev.* **2000**, *100*, 3963.
(39) Pino, T.; Boudin, N.; Brechignac, P. *J. Chem. Phys.* **1999**, *111*, 7337.
(40) Piest, H.; von Helden, G.; Meijer, G. *J. Chem. Phys.* **1999**, *110*, 2010.
(41) Fujii, A.; Fujimaki, E.; Ebata, T.; Mikami, N. *J. Chem. Phys.* **2000**, *112*, 6275.
(42) Bieske, E. J. *J. Chem. Soc., Faraday Trans.* **1995**, *91*, 1.
(43) Nizkorodov, S. A.; Dopfer, O.; Ruchti, T.; Meuwly, M.; Maier, J. P.; Bieske, E. J. *J. Phys. Chem.* **1995**, *99*, 17118.
(44) NIST Chemistry Web Book; http:/webbook.nist.gov 2001.
(45) Frisch, M. J.; Trucks, G. W.; Schlegel, H. B.; Scuseria, G. E.; Robb, M. A.; Cheeseman, J. R.; Zakrzewski, V. G.; Montgomery, J. A.; Stratman, R. E.; Burant, J. C.; Dapprich, S.; Millam, J. M.; Daniels, A. D.; Kudin, K. N.; Strain, M. C.; Farkas, O.; Tomasi, J.; Barone, V.; Cossi, M.; Cammi, R.; Menucci, B.; Pomelli, C.; Adamo, C.; Clifford, S.; Ochterski, J.; Petersson, G. A.; Ayala, P. Y.; Cui, Q.; Morokuma, K.; Malick, D. K.; Rabuck, D.; Raghavachari, K.; Foresman, J. B.; Cioslowski, J.; Ortiz, J. V.; Stefanov, B. B.; Liu, G.; Liashenko, A.; Piskorz, P.; Komaromi, I.; Gomperts, R.; Martin, R. L.; Fox, D. J.; Keith, T.; Al-Laham, M. A.; Peng, C. Y.; Nanayakkara, A.; Gonzales, C.; Challacombe, M.; Gill, P. M. W.; Johnson, B. G.; Chen, W.; Wong, M. W.; Andres, J. L.; Gonzales, C.; Head-Gordon, M.; Replogle, E. S.; Pople, J. A. *Gaussian 98*, Revision A.5; Gaussian, Inc.: Pittsburgh, PA, 1998.
(46) Boys, S. F.; Bernardi, F. *Mol. Phys.* **1970**, *19*, 553.

are only slightly modified upon N_2 complexation, the nomenclature employed for the normal modes of $C_3H_3^+$-N_2 refers to the intramolecular modes of $C_3H_3^+$ (ν_i), the N_2 stretch vibration (ν_{N-N}), and the intermolecular bending and stretching modes (ν_b, ν_s), respectively. A figure of the normal modes of c-$C_3H_3^+$ may be found in ref 28.

In agreement with previous calculations, c-$C_3H_3^+$ (D_{3h}) is found to be the most stable isomer of $C_3H_3^+$. The calculated equilibrium geometry (Figure 1) and harmonic vibrational frequencies (Table 1) are also in satisfying agreement with available experimental and theoretical data. The global minimum on the intermolecular potential of c-$C_3H_3^+$-N_2 corresponds to the planar H-bound structure, in which the N_2 ligand forms a linear ionic hydrogen bond to one of the three equivalent protons of c-$C_3H_3^+$ (Figure 1, C_{2v}). The intermolecular bond is characterized by a dissociation energy of $D_e = 1227$ cm^{-1}, an intermolecular H−N separation of $R_e = 2.1772$ Å, and a harmonic intermolecular stretching frequency of $\omega_s = 108$ cm^{-1}. As expected, the major effect of N_2 complexation on the c-$C_3H_3^+$ ion is an elongation of the C−H bond adjacent to the intermolecular bond ($\Delta r_e = 0.005$ Å). The calculated equilibrium structure of c-$C_3H_3^+$-N_2 is close to a prolate symmetric top ($\kappa_e = -0.996$), with rotational constants of $A_e = 1.0326$ cm^{-1}, $B_e = 0.0455$ cm^{-1}, and $C_e = 0.0436$ cm^{-1}. In general, the intermolecular bond has only modest effects on the vibrational frequencies and IR intensities. Most relevant for the present work are the effects on the C−H stretch fundamentals. Complexation reduces the symmetry from D_{3h} for c-$C_3H_3^+$ to C_{2v} for H-bound c-$C_3H_3^+$-N_2. As a consequence, the IR forbidden symmetric stretch vibration, $\nu_1(a_1)$, becomes IR allowed in the complex (mainly a symmetric linear combination of the two free C−H stretch local modes). Its IR intensity, however, remains rather weak. More importantly, the degenerate antisymmetric C−H stretch, $\nu_4(e')$, splits into two components in the dimer, $\nu_4(a_1)$ and $\nu_4(b_2)$. The $\nu_4(a_1)$ mode is predominantly the bound C−H stretch and experiences thus a significant red shift upon formation of the proton bond, $\Delta\nu_4(a_1) = -59$ cm^{-1}. On the other hand, the $\nu_4(b_2)$ mode is mainly an antisymmetric linear combination of the free C−H stretch modes and experiences only a very small blue shift, $\Delta\nu_4(b_2) = +3$ cm^{-1}.

The three equivalent H-bound global minima are not the only minima located on the intermolecular potential of c-$C_3H_3^+$-N_2. The nonplanar C-bound structures in which the N_2 ligand is situated above the aromatic $C_3H_3^+$ ring and pointing toward one of the C atoms (C_s) are local minima ($D_e = 1102$ cm^{-1}). The planar side-bound structures in which N_2 is pointing toward the midpoint of a C−C bond of c-$C_3H_3^+$ are transition states (C_{2v}) connecting two equivalent H-bound global minima. Their dissociation energy of 923 cm^{-1} corresponds to a 3-fold barrier of 304 cm^{-1} to in-plane internal rotation of c-$C_3H_3^+$. As this barrier is much higher than the effective internal rotor constant ($b_{eff} \approx C_{c-C_3H_3^+} \approx 0.5$ cm^{-1}), this hindered internal motion is largely quenched. The π-bound structure in which N_2 approaches c-$C_3H_3^+$ along its C_3 symmetry axis is a second-order transition state (C_{3v}, $D_e = 995$ cm^{-1}) with a similar energy as the C-bound local minimum. This implies that the potential above the aromatic ring is rather flat. The C-bound, π-bound, and side-bound structures can easily be distinguished from the H-bound minima by their characteristic C−H stretch frequencies (shifts, splittings, IR intensities) and their rotational constants.

The H_2CCCH^+ isomer of $C_3H_3^+$ (Figure 1) is calculated to be 31.5 kcal/mol less stable than c-$C_3H_3^+$ (including harmonic zero-point corrections), in reasonable agreement with the experimental value (≈25 kcal/mol).[2] Similar to c-$C_3H_3^+$, the calculated structure (Figure 1) and vibrational frequencies (Table 1) are in good agreement with available experimental and theoretical studies. The global minimum on the intermolecular potential of H_2CCCH^+-N_2 corresponds to a H-bound structure, in which the N_2 ligand forms a linear ionic hydrogen bond to the acetylenic proton of H_2CCCH^+ (Figure 1, C_{2v}). The intermolecular bond in H_2CCCH^+-N_2 ($D_e = 1373$ cm^{-1}, $R_e = 2.0916$ Å, $\omega_s = 120$ cm^{-1}) is slightly stronger and shorter compared to that in c-$C_3H_3^+$-N_2, as the proton affinity of H_2CCC is lower than that of c-C_3H_2.[18] Similar to c-$C_3H_3^+$-N_2, the H_2CCCH^+-N_2 dimer has an equilibrium structure close to a prolate symmetric top ($A_e = 9.5832$ cm^{-1}, $B_e = 0.0356$ cm^{-1}, $C_e = 0.0355$ cm^{-1}, $\kappa_e = -0.99996$). As expected, the largest effect of N_2 complexation is an elongation of the acetylenic C−H bond ($\Delta r_e = 0.008$ Å), leading to a large red shift of the corresponding strongly IR active C−H stretch frequency ($\Delta\nu_1 = -115$ cm^{-1}) and a significant enhancement in its IR intensity (factor 4). In addition, the in-plane and out-of-plane bending fundamentals of the acetylenic C−H bond experience a large blue shift upon complexation ($\Delta\nu_{11} = +119$ cm^{-1}, $\Delta\nu_7 = +93$ cm^{-1}), due to the additional retarding forces arising from the intermolecular bond. The other frequencies are less affected ($|\Delta\nu_i| < 30$ cm^{-1}, Table 1). Experimentally, only the H-bound H_2CCCH^+-N_2 global minimum of the interaction potential between N_2 and H_2CCCH^+ is observed. Thus, properties of other local minima (e.g., the isomer in which N_2 binds to one of the protons of the CH_2 group, $D_e = 1180$ cm^{-1}) are not discussed in detail further.

In general, the weak intermolecular interaction has little influence on the properties of the N_2 ligand (Figure 1, Table 1). The calculations predict for bare N_2 an interatomic separation of 1.1108 Å and a harmonic frequency of 2204 cm^{-1}. In H-bound H_2CCCH^+-N_2, the N−N bond becomes slightly stronger and shorter ($\Delta r_e = -0.0007$ Å), leading to a blue shift in the N−N stretch frequency ($\Delta\nu_{N-N} = +7$ cm^{-1}). Similar trends are observed in H-bound c-$C_3H_3^+$-N_2 ($\Delta r_e = -0.0004$ Å, $\Delta\nu_{N-N} = +4$ cm^{-1}), although the effects are less pronounced owing to the somewhat weaker interaction.

IV. Experimental Results and Discussion

Figure 3 shows the overview spectrum of the $C_3H_3^+$-N_2 dimer in the range between 2970 and 3370 cm^{-1} and an expanded view between 3050 and 3150 cm^{-1}. In total, eight vibrational transitions are observed in this spectral range and they are denoted A−H. Their rotational structures are appropriate for either parallel ($\Delta K_a = 0$) or perpendicular ($\Delta K_a = \pm 1$) transitions of (near) symmetric prolate tops. The band centers and their suggested assignments are summarized in Table 2. Two Q branch series corresponding to perpendicular transitions are clearly identified (bands C and E): the approximate spacings of adjacent Q branches, $2(A - B) \approx 2A$ (because $B \ll A$), are largely different for both series (≈16.5 and ≈2 cm^{-1}, respectively), indicating the presence of at least two $C_3H_3^+$-N_2 isomers. By comparison with the ab initio calculations, they can unambiguously be assigned to the H-bound dimers of c-$C_3H_3^+$-N_2 ($A \approx 1$ cm^{-1}) and H_2CCCH^+-N_2 ($A \approx 8.5$ cm^{-1}) shown in Figure 1.

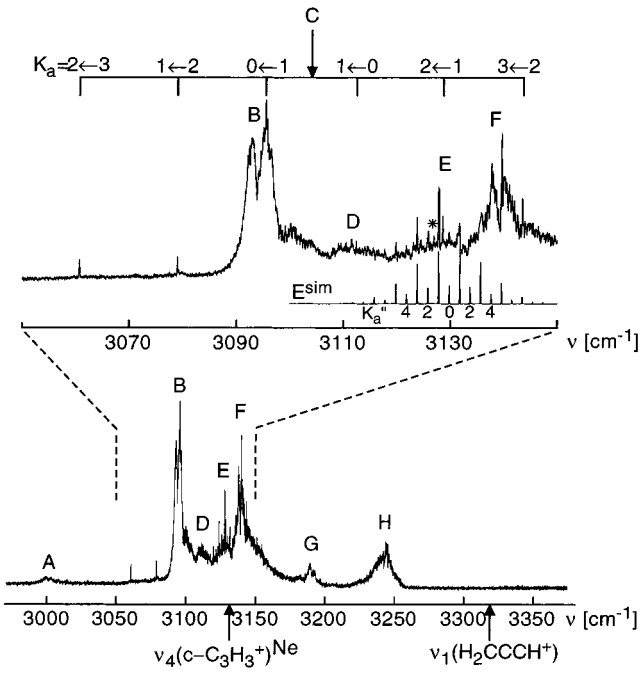

Figure 3. Overview of the IR photodissociation spectrum of $C_3H_3^+$-N_2 ionic complexes recorded between 2970 and 3370 cm^{-1}. An expanded view of the range between 3050 and 3150 is shown as well. The observed transitions are labeled A−H and their positions and assignments are listed in Table 2. The arrows below the wavenumber axis indicate the positions of the gas-phase ν_1 frequency of H_2CCCH^+ (ref 9) and the ν_4 frequency of c-$C_3H_3^+$ measured in a Ne matrix (ref 10). The K_a assignments of the two perpendicular transitions C and E are indicated (Tables 3 and 4). A simulation of transition E with the molecular parameters described in the text (E^{sim}) is included for a comparison with the experimental transition.

Table 2. Positions (in cm^{-1}), Widths (fwhm, in parentheses), and Suggested Assignments of the Observed Transitions in the IR Spectrum of $C_3H_3^+$-N_2 (Figure 3)

transition	position	type	isomer	assignment
A	3001 (6)	∥	H_2CCCH^+-N_2	$2\nu_4$
B	3093.9 (5.4)	∥	c-$C_3H_3^+$-N_2	$\nu_4(a_1)$
C	3104.91[a]	⊥	H_2CCCH^+-N_2	$\nu_3+\nu_{7/10}$
D	3113 (10)	∥	H_2CCCH^+-N_2	ν_2
E	3128.75[a]	⊥	c-$C_3H_3^+$-N_2	$\nu_4(b_2)$
F	3139 (4)	∥	H_2CCCH^+-N_2	ν_1
G	3190.5 (6)	∥	H_2CCCH^+-N_2	$\nu_3+\nu_5$?
H	3243 (13)	∥	H_2CCCH^+-N_2	$\nu_3+\nu_5$?

[a] For the perpendicular transitions C and E the fitted band origin ν_0 is listed.

A. The ν_4 vibration of H-Bound c-$C_3H_3^+$-N_2. According to the calculations for c-$C_3H_3^+$-N_2 (Table 1) and previous spectra of c-$C_3H_3^+$ in salt crystals, SO_2 solutions, and Ne matrices, only the strongly IR active C−H stretch fundamental ν_4 of c-$C_3H_3^+$-N_2 is expected to occur with significant intensity in the spectral range covered in Figure 3.[1,4,10] The ν_4 frequency of bare c-$C_3H_3^+$ has not been measured in the gas phase. Measurements in a Ne matrix and in SO_2 solution yield 3130.4 and 3138 cm^{-1}, respectively.[4,10] As outlined in section III, symmetry reduction from D_{3h} to C_{2v} causes the $\nu_4(e')$ fundamental of c-$C_3H_3^+$ to split into two components in H-bound c-$C_3H_3^+$-N_2 (Table 1): a perpendicular component with a small blue shift, $\nu_4(b_2)$, and a parallel component with a larger red shift, $\nu_4(a_1)$. Closer inspection of the IR spectrum of $C_3H_3^+$-N_2 in Figure 3 reveals two strong transitions in the corresponding frequency range, which have the appropriate rotational structures

Table 3. Positions (in cm^{-1}), Widths (fwhm, in parentheses), and Assignments of the Q Branches of the $\nu_4(b_2)$ Transition of H-Bound c-$C_3H_3^+$-N_2 (band E)

position[a]	$K_a' \leftarrow K_a''$	position[a]	$K_a' \leftarrow K_a''$
3119.78 (0.06)	4 ← 5	3129.73 (0.19)	1 ← 0
3121.76 (0.10)	3 ← 4	3131.69 (0.13)	2 ← 1
3123.78 (0.07)	2 ← 3	3135.62 (0.17)	4 ← 3
3125.79 (0.16)	1 ← 2	3137.62 (0.07)	5 ← 4
3127.77 (0.06)	0 ← 1	3139.56 (0.09)	6 ← 5
		3143.40 (0.09)	8 ← 7

[a] Absolute accuracy of calibration is 0.02 cm^{-1}.

required for $\nu_4(a_1)$ and $\nu_4(b_2)$ of H-bound c-$C_3H_3^+$-N_2. The parallel transition at 3094 cm^{-1} (band B) and the perpendicular transition centered near 3129 cm^{-1} (band E) can safely be assigned to $\nu_4(a_1)$ and $\nu_4(b_2)$ of H-bound c-$C_3H_3^+$-N_2, respectively. The observed splitting (35 cm^{-1}) and intensity ratio of $\nu_4(b_2)$ and $\nu_4(a_1)$ are in qualitative agreement with the ab initio predictions (Table 1).

Individual $\Delta K_a = 0$ subbands of the parallel $\nu_4(a_1)$ band strongly overlap, leading to the appearance of a nearly symmetric band contour with single unresolved P, Q, and R branches. The $\nu_4(a_1)$ band center is estimated to be close to the band gap (3093.9 cm^{-1}) and is shifted 37 cm^{-1} to the red of the Ne matrix value of c-$C_3H_3^+$ (indicated by an arrow in Figure 3). The width of the band ($\approx$5 cm^{-1}) is compatible with the rotational constants determined by the ab initio calculations in section III and a rotational temperature of $\approx$30 K. The latter value is consistent with the simulations of the perpendicular transitions (discussed below) and typical for cluster ions produced in this ion source.[47,48] Closer inspection shows that the $\nu_4(a_1)$ band is slightly shaded to the blue, indicating that the rotational constants increase slightly upon vibrational excitation. This observation is expected because $\nu_4(a_1)$ corresponds mainly to a stretching of the C−H bond acting as the proton donor in the intermolecular bond. In general, excitation of such proton donor stretches in H-bound dimers leads to an increase of the intermolecular interaction strength, with the consequence of a shorter intermolecular bond (i.e., larger rotational constants) and a red shift in the proton stretch frequency.[38,48,49]

In contrast to $\nu_4(a_1)$, individual Q branches of the $\Delta K_a = \pm 1$ subbands of the perpendicular $\nu_4(b_2)$ transition (band E) are clearly discernible (Figure 3). The positions and widths of the eleven Q branches observed are listed in Table 3 along with their suggested assignments. Adjacent Q branches are spaced by $2A \approx 2$ cm^{-1}, consistent with the calculated A rotational constant of H-bound c-$C_3H_3^+$-N_2 ($A_e = 1.0326$ cm^{-1}). Moreover, alternating Q branches display the distinct intensity alternation expected for two equivalent protons: the nuclear spin statistical weights are 1 (para) and 3 (ortho) for rotational levels with even and odd K_a values (having A and B rotational symmetry in C_{2v}).[50] On the basis of the K_a assignments given in Table 3 and Figure 3, the Q branch positions are least-squares fitted to a standard Hamiltonian appropriate for a rigid near symmetric prolate top:[51]

(47) Roth, D.; Dopfer, O.; Maier, J. P. *Phys. Chem. Chem. Phys.* **2001**, *3*, 2400.
(48) Dopfer, O.; Roth, D.; Maier, J. P. *J. Phys. Chem. A* **2000**, *104*, 11702.
(49) Olkhov, R. V.; Dopfer, O. *Chem. Phys. Lett.* **1999**, *314*, 215.
(50) Herzberg, G. *Molecular Spectra and Molecular Structure. II. Infrared and Raman Spectra of Polyatomic Molecules*; Krieger Publishing Company: Malabar, FL, 1991.

$$\hat{H} = \nu_0 + \bar{B}J(J+1) + (A - \bar{B})K_a^2 \quad (1)$$

Using the approximation $\bar{B}' \approx \bar{B}'' \approx \bar{B}_e = (B_e + C_e)/2$ and taking the ab initio value $\bar{B}_e = 0.04456$ cm^{-1}, the following molecular constants are obtained: $\nu_0 = 3128.747(9)$ cm^{-1}, $A'' = 1.0365(12)$ cm^{-1}, and $A' = 1.0332(9)$ cm^{-1}. As expected, the A rotational constant decreases slightly upon $\nu_4(b_2)$ excitation, due to an effective lengthening of the free C−H bonds (this normal mode corresponds mainly to the antisymmetric linear combination of the two free C−H stretch local modes). The standard deviation of the fit ($\sigma = 0.02$ cm^{-1}) is consistent with the typical width of the unresolved Q branches (0.06−0.19 cm^{-1}). A simulation of $\nu_4(b_2)$ using the derived molecular constants, a rotational temperature of 30 K, and a convolution width of 0.08 cm^{-1} is included in Figure 3 (E^{sim}) and shows good agreement with the experimental spectrum (band E). The assignment of the K_a quantum numbers in Table 3 and Figure 3 is based on the relative Q branch intensities averaged over more than 10 individual scans. Although the given assignment is strongly favored, it cannot be completely ruled out that it may be shifted by two Q branches to lower energy. The main effect of such a reassignment would be a red shift in the band origin of $\nu_4(b_2)$ by ca. −4 cm^{-1}. The calculations suggest that the complexation-induced frequency shift is less than +4 cm^{-1}. Thus, using the favored assignment for $\nu_4(b_2)$, the gas-phase value of the ν_4 fundamental of bare c-$C_3H_3^+$ can be estimated as 3127 ± 2 cm^{-1}. For the alternative assignment, the estimate would be 3123 ± 2 cm^{-1}. Both values are compatible with the Ne matrix value of 3130.4 ± 1 cm^{-1}.[10] For comparison, the best values derived from ab initio anharmonic force fields are 3178 and 3149 cm^{-1}.[27,28]

The rovibrational analysis (nuclear spin statistical weights, magnitude and direction of vibrational band shifts and splittings, IR intensities, and rotational constants) clearly show that the H-bound global minimum of c-$C_3H_3^+$-N_2 is the only c-$C_3H_3^+$-N_2 isomer detected in the spectrum in Figure 3. This observation is in agreement with the calculations described in section III, which predict that the side-bound and π-bound isomers of c-$C_3H_3^+$-N_2 are not minima on the intermolecular potential but transition states. The population of the C-bound local minima is below the detection limit, probably because of the low isomerization barrier toward the H-bound global minima. In addition, vibrational band shifts and splittings as well as photofragmentation branching ratios measured in the spectra of larger $C_3H_3^+$-$(N_2)_n$ clusters ($n = 2-6$) confirm the assignments of bands B and E to $\nu_4(a_1)$ and $\nu_4(b_2)$ of c-$C_3H_3^+$-N_2.[52] Moreover, these spectra show that all other bands observed in Figure 3 are not arising from c-$C_3H_3^+$-N_2, but from other $C_3H_3^+$-N_2 complexes.[52]

B. The ν_1 Vibration of H-Bound H_2CCCH^+-N_2. The rovibrational analysis of band C in the spectrum of $C_3H_3^+$-N_2 (Figure 3) discussed in section IV.C gives unambiguous proof of the presence of H_2CCCH^+ and its H-bound H_2CCCH^+-N_2 dimer (Figure 1) in the expansion. According to the ab initio data (Table 1), ν_1 is by far the strongest IR active fundamental of this dimer in the spectral range investigated. It corresponds to the stretching mode of the acetylenic C−H bond adjacent to the intermolecular proton bond. For free H_2CCCH^+, the gas-phase frequency of this mode has been derived from the zero-kinetic-energy (ZEKE) photoelectron spectrum of H_2CCCH as $\nu_1 = 3319$ cm^{-1} (indicated by an arrow in Figure 3). As no intense absorption is observed in the IR spectrum of $C_3H_3^+$-N_2 within 80 cm^{-1} of this value, the ν_1 fundamental of any H_2CCCH^+-N_2 isomer present in the expansion has to feature a substantial complexation shift, $\Delta\nu_1$. This can only occur when the N_2 ligand binds to the terminal, acetylenic C−H group of H_2CCCH^+. Consequently, the H-bound H_2CCCH^+-N_2 dimer shown in Figure 1 is the only H_2CCCH^+-N_2 isomer present in the expansion. This observation is consistent with the ab initio data, which predict that this structure is the global minimum of this dimer. According to the calculations (Table 1), the ν_1 vibration of H-bound H_2CCCH^+-N_2 features a large red shift (−115 cm^{-1}) and a strong enhancement in its IR intensity (factor 4). Band F centered at 3139 cm^{-1} in the spectrum of $C_3H_3^+$-N_2 (Figure 3) is the strongest transition observed in the corresponding frequency range and thus assigned to ν_1 of H-bound H_2CCCH^+-N_2. The observed red shift upon complexation (−180 cm^{-1} or 5.42%) is somewhat larger than the predicted value (−115 cm^{-1} or 3.37%), implying that the MP2(full)/6-311G(2df,2pd) level underestimates the interaction strength and the frequency shift. The band contour is appropriate for a parallel transition of a near-symmetric prolate top with overlapping $\Delta K_a = 0$ subbands. Moreover, the band is strongly blue shaded, which is a typical signature of the excitation of a proton donor stretch in H-bound dimers (as outlined earlier for $\nu_4(a_1)$ of c-$C_3H_3^+$-N_2). Spectra of larger $C_3H_3^+$-$(N_2)_n$ clusters ($n = 2-6$) display significant monotonic incremental blue shifts of this transition as the cluster size increases.[52] A similar behavior has previously been observed for $SiOH^+$-$(N_2)_n$ complexes[53] and is typical for solvation of a H-bound AH^+-L dimer with further ligands L around the linear AH^+-L proton bond.[43,53−55] It strongly supports the assignment of band F to ν_1 of H-bound H_2CCCH^+-N_2. All spectral observations discussed for band F rule out that bands G or H can be assigned to this vibration.[52]

C. Other Vibrations of H-Bound H_2CCCH^+-N_2. In contrast to the bands B, E, and F, the vibrational assignments of the other transitions are less certain. As argued in section IV.A, they are almost certainly not due to a c-$C_3H_3^+$-N_2 dimer.[56] Moreover, they cannot originate from any non-H-bound H_2CCCH^+-N_2 dimer (section IV.B). Thus, they have probably all to be attributed to the H-bound H_2CCCH^+-N_2 dimer and this scenario is assumed for the following discussion.

Band C has the rotational structure appropriate for a perpendicular transition of a near symmetric prolate top (Figure 3). Six unresolved Q branches are observed and their averaged spacing of $2A \approx 16.5$ cm^{-1} corresponds to an A rotational constant of ≈8.3 cm^{-1}. This transition can therefore unambiguously be attributed to the H-bound H_2CCCH^+-N_2 dimer, having only two H atoms displaced from the a-axis. The calculated A constant of the equilibrium structure (Figure 1), $A_e = 9.5832$ cm^{-1}, is somewhat larger than the observed value, probably because of the large zero-point effects of the light H atoms on

(51) Herzberg, G. *Molecular Spectra and Molecular Structure. III. Electronic Spectra and Electronic Structure of Polyatomic Molecules*; Krieger Publishing Company: Malabar, FL, 1991.
(52) Roth, D. Ph.D. Thesis, University of Basel 2001.
(53) Olkhov, R. V. Ph.D. Thesis, University of Basel, 1999.
(54) Olkhov, R. V.; Nizkorodov, S. A.; Dopfer, O. *Chem. Phys.* **1998**, *239*, 393.
(55) Dopfer, O.; Olkhov, R. V.; Maier, J. P. *J. Phys. Chem. A* **1999**, *103*, 2982.
(56) Roth, D.; Dopfer, O. Unpublished results, 2000.

Table 4. Positions (in cm^{-1}), Widths (fwhm, in parentheses), and Assignments of the Q Branches of Band C (assigned to $\nu_3 + \nu_{7/10}$) of H-Bound H_2CCCH^+-N_2

position[a]	$K_a' \leftarrow K_a''$
3060.86 (0.13)	2 ← 3
3079.12 (0.07)	1 ← 2
3195.9[b] (0.13)	0 ← 1
3112.48 (0.07)	1 ← 0
3128.56 (0.06)	2 ← 1
3143.40 (0.09)	3 ← 2

[a] Absolute accuracy of calibration is 0.02 cm^{-1}. [b] Uncertainty in position is 0.5 cm^{-1} due to calibration problems.

the *A* constant even in the ground vibrational state. The positions and widths of the observed Q branches are listed in Table 4 along with their assignments. Alternating Q branches display the proper intensity alternation expected from the nuclear spin statistical weights of 1 and 3 for rotational levels with even and odd K_a values (i.e., levels of A and B rotational symmetry in C_{2v}).[50] A least-squares fit of four Q branch positions to Hamiltonian (1) using the ab initio value $\bar{B}_e = 0.035566$ cm^{-1} leads to $\nu_0 = 3104.91(7)$ cm^{-1}, $A'' = 8.499(9)$ cm^{-1}, and $A' = 8.073(9)$ cm^{-1} (the $K_a = 1 \leftarrow 0$ and $0 \leftarrow 1$ Q branches are not included in the fit due to calibration difficulties and a local perturbation). The standard deviation of the fit ($\sigma = 0.03$ cm^{-1}) is compatible with the typical width of the Q branches (0.06−0.13 cm^{-1}). Simulations of the Q branch intensities are consistent with a rotational temperature of ≈40 K.

Assuming that band C originates from the vibrational ground state of H-bound H_2CCCH^+-N_2, the assignment of the upper level has to satisfy following conditions: (i) the observation of a perpendicular transition requires that the vibrational symmetry species of the upper level is either b_1 or b_2; (ii) the *A* rotational constant must decrease significantly upon vibrational excitation (the observed decrease is 5%); (iii) its IR intensity must be sufficiently large to be observed in the spectrum in Figure 3; and (iv) the frequency has to match 3105 cm^{-1}. After inspection of Table 1, the first obvious candidate to be considered is the antisymmetric C−H stretch fundamental of the CH_2 group, $\nu_9(b_2)$, which fulfills criteria i−iii. However, the calculations predict its frequency to be ≈100 cm^{-1} higher than the corresponding symmetric C−H stretch, $\nu_2(a_1)$. As both of them are not sensitive to N_2 complexation, the experimental value for $\nu_9(b_2)$ of H_2CCCH^+-N_2 can be estimated as ≈3230 cm^{-1} from the measured $\nu_2(a_1)$ frequency of bare H_2CCCH^+ (3130 cm^{-1})[9] and is thus too high to be responsible for band C at 3105 cm^{-1}. As no other fundamental with b_1 or b_2 symmetry is in the 3000 cm^{-1} range, combination bands are considered. The $\nu_3(a_1)$ mode of H_2CCCH^+ corresponds to the acetylenic C−C stretch with a frequency of ≈2100 cm^{-1}.[9,10] This mode has by far the largest IR oscillator strength[10,31] and complexation with N_2 enhances its intensity by 50% (Table 1). Thus, combination bands of $\nu_3(a_1)$ with other vibrations having a frequency of ≈1000 cm^{-1} may be expected in the 3100 cm^{-1} range. According to this scenario, the most probable candidates for band C are the combination bands $\nu_3 + \nu_7(b_1)$ and $\nu_3 + \nu_{10}(b_2)$. The $\nu_7(b_1)$ mode is the out-of-plane bending vibration of the acetylenic C−H bond: its frequency has been estimated for free H_2CCCH^+ as 910 cm^{-1} and the calculations predict a blue shift of ≈90 cm^{-1} upon complexation with N_2 (Table 1). The $\nu_{10}(b_2)$ mode (CH_2 in-plane bending mode) with a calculated frequency of 1050 cm^{-1} is the only other vibration with b symmetry in the 1000 cm^{-1} range. Hence, at the present stage, an assignment of band C to either $\nu_3 + \nu_7(b_1)$ or $\nu_3 + \nu_{10}(b_2)$ is favored (Table 2).

The four remaining bands (A, D, G, H) are parallel transitions, that is the symmetry species of the upper level has to be a_1 (under the assumption that they originate from the ground state of H-bound H_2CCCH^+-N_2). A reasonable assignment for the weak transition A at 3001 cm^{-1} is to the overtone of the symmetric in-plane CH_2 bending vibration, $2\nu_4(a_1)$. Its fundamental frequency has been measured as 1465 cm^{-1} for bare H_2CCCH^+.[9] As the ν_4 mode does not shift upon N_2 complexation, the assignment of band A to $2\nu_4(a_1)$ implies a significant positive anharmonicity ($2\nu_4 - \nu_4 - \nu_4 = 3001 - 2 \times 1465 = 71$ cm^{-1}). The weak band D at 3113 cm^{-1} is attributed to the symmetric C−H stretching vibration of the CH_2 group, $\nu_2(a_1)$. The monomer transition is reported as ≈3130 cm^{-1} (with an uncertainty of ±10 cm^{-1})[9] and the predicted complexation shift is small (Table 1). One out of the two bands G (3190.5 cm^{-1}) and H (3243 cm^{-1}) is attributed to $\nu_3 + \nu_5(a_1)$, a combination tone of the two C−C stretch modes of H_2CCCH^+. As mentioned before, owing to the large IR oscillator strength of ν_3, combination bands of ν_3 with other modes are expected in the IR spectrum. On the basis of the ZEKE spectrum, the frequency of $\nu_3 + \nu_5$ is estimated as $2122 + 1106 = 3228$ cm^{-1} in free H_2CCCH^+ (neglecting cross anharmonicities).[9] Taking the calculated N_2 complexation shift into account (−15 cm^{-1}, Table 1), $\nu_3 + \nu_5$ of H-bound H_2CCCH^+-N_2 is expected near 3213 cm^{-1}, in agreement with the observed frequencies of both band G (3190.5 cm^{-1}) and band H (3243 cm^{-1}). Other options for these two bands are not obvious and may involve higher order combination bands. Spectra of larger $C_3H_3^+$-$(N_2)_n$ complexes as well as other $C_3H_3^+$-L dimers (L = Ne, Ar, O_2, CO_2) show that the positions of both bands are relatively insensitive to the type of ligand and the degree of solvation.[52] Moreover, the two bands are also very weakly observed in some Ne matrix spectra when ions with the mass of $C_3H_3^+$ are deposited.[57] Thus, they cannot be attributed to combination bands of the intense ν_1 fundamental of H_2CCCH^+-N_2 with a low-frequency intermolecular mode (ν_s or ν_b), because such transitions would be very sensitive to solvation. Strong $\nu_1 + \nu_{s/b}$ combination bands are often observed in the IR spectra of H-bound dimers.[48,54,55,58] Possibly, one of the two bands G and H is due to a C−H stretching vibration of a $C_3H_3^+$-N_2 dimer involving the less stable H_2CCHC^+ or H_3CCC^+ core ions. Another possibility is that dimers of the type $[C_2NH]^+$-N_2 may contribute to the $C_3H_3^+$-N_2 spectra, as $[C_2NH]^+$ ions have the same mass as $C_3H_3^+$. Isomeric $[C_2NH]^+$ ions may be produced in the ion source via ion−molecule reaction chemistry of the $H_2CCCH_2/N_2/Ar$ mixture, owing to the large N_2 concentration. However, this scenario is unlikely because the two bands G and H occur also with similar relative intensities in the IR spectra of $C_3H_3^+$-L dimers with L ≠ N_2 and in the Ne matrix spectrum of $C_3H_3^+$, where N_2 could occur only as impurity in the ion source.

In addition to bands A−H discussed so far, two further transitions are observed in the IR spectrum of $C_3H_3^+$-N_2. A single Q branch at 3126.91 cm^{-1} (width 0.06 cm^{-1}) in the vicinity of band E (indicated by an asterisk in Figure 3) cannot

(57) Wyss, M. Ph.D. Thesis, University of Basel, 2001.
(58) Dopfer, O.; Olkhov, R. V.; Roth, D.; Maier, J. P. *Chem. Phys. Lett.* **1998**, *296*, 585.

be assigned to any of the perpendicular transitions described above. Depending on the assignment of band C to either $\nu_3 + \nu_7$ or $\nu_3 + \nu_{10}$ of H-bound H_2CCCH^+-N_2, this Q branch may be attributed to the other alternative. The second band occurs near 6174 cm^{-1} and is a parallel transition (width 6 cm^{-1}). It is only observed in scans where, in addition to the idler output of the OPO (2500−4500 cm^{-1}), radiation of the signal output (4900−6800 cm^{-1}) could interact with the $C_3H_3^+$-N_2 ion beam. It is probably arising from a C−H stretching overtone of either H_2CCCH^+-N_2 or c-$C_3H_3^+$-N_2. Clearly, a definitive assignment of the bands other than B, E, and F requires further spectroscopic studies (in particular using isotopic substitution) and/or higher level theoretical data.

D. Structure and Abundance of c-$C_3H_3^+$ and H_2CCCH^+. In this section, some conclusions about the properties of H_2CCCH^+ and c-$C_3H_3^+$ are derived from the rovibrational spectra of their N_2 dimers. As both H_2CCCH^+ and c-$C_3H_3^+$ have not been characterized by spectroscopy at the level of rotational resolution, the dimer spectra in Figure 3 provide the first experimental structural information for these important hydrocarbon cations in the gas phase. The *A* rotational constants and nuclear spin statistical weights derived from the rovibrational analysis of the bands assigned to H_2CCCH^+-N_2 and c-$C_3H_3^+$-N_2 unambiguously show that both complexes have C_{2v} symmetry (Figure 1) with two equivalent H atoms and linear intermolecular −C−H···N−N bonds. The large observed *A* constant of H_2CCCH^+-N_2 ($A'' \approx 8.5$ cm^{-1}) implies that only the two H atoms of the CH_2 group are displaced from the *a*-axis of the complex. This observation provides the first experimental proof for the planar C_{2v} structure of the H_2CCCH^+ monomer with a linear C−C−C−H backbone (Figure 1). The only previous and tentative spectroscopic evidence for such a H_2CCCH^+ structure comes from the vibrational analysis of the low-resolution ZEKE spectrum of H_2CCCH.[9] Previous high-level ab initio calculations also predict a C_{2v} geometry for H_2CCCH^+ (in excellent agreement with the geometry in Figure 1).[30] The calculations show that N_2 complexation has practically no influence on the *A* rotational constant: $A_e = 9.5832$ and 9.5797 cm^{-1} for H_2CCCH^+-N_2 and H_2CCCH^+ (i.e., $\Delta A_e = 0.0035$ cm^{-1} or 0.04%). Hence, the ground-state value derived for H_2CCCH^+-N_2 ($A'' = 8.499$ cm^{-1}) should be very close to the one for free H_2CCCH^+. Similarly, the spectrum of c-$C_3H_3^+$-N_2 strongly supports the planar D_{3h} symmetric structure of free c-$C_3H_3^+$ predicted by ab initio calculations and the analysis of low-resolution IR and Raman spectra of c-$C_3H_3^+X^-$ in the condensed phase.[4] The calculations yield $A_e = 1.0326$ and 1.0306 cm^{-1} for c-$C_3H_3^+$-N_2 and c-$C_3H_3^+$ ($\Delta A_e = 0.002$ cm^{-1} or 0.2%), so that the ground-state value of c-$C_3H_3^+$-N_2, $A'' = 1.0365$ cm^{-1}, provides a good estimate for the corresponding c-$C_3H_3^+$ value.

The relative band intensities observed in the IR spectra of H_2CCCH^+-N_2 and c-$C_3H_3^+$-N_2 can be used to roughly estimate the relative abundance of H_2CCCH^+ and c-$C_3H_3^+$ in the allene/N_2/Ar plasma expansion using the following information and approximations. The observed intensity ratio of $\nu_4(a_1)$ of c-$C_3H_3^+$-N_2 and ν_1 of H_2CCCH^+-N_2 is ≈2 (Figure 3). The ratio of the theoretical IR oscillator strengths of both bands is nearly unity (0.75, Table 1). The probability of forming N_2 complexes is assumed to be roughly the same for both $C_3H_3^+$ monomers due to their similar theoretical association energies. On the basis of this crude model, the number density of c-$C_3H_3^+$ is estimated to be about twice that of H_2CCCH^+. As mentioned in section II, the IR spectra are nearly independent of using allene, propyne, 3-chloro-1-propyne, or benzene as precursor. Previous reactivity studies have shown that electron impact ionization of propyne forms a mixture of the two $C_3H_3^+$ isomers in the ratio of ≈60% c-$C_3H_3^+$ and ≈40% H_2CCCH^+,[6] in excellent agreement with the present experiments with allene.

E. Comparison to Other AH^+-N_2 Complexes. The attractive long-range part of the intermolecular interaction in weakly bound AH^+-N_2 dimers is dominated by the electrostatic and inductive interactions between the positive charge distribution in AH^+ and the negative quadrupole moment and the anisotropic polarizability of N_2. The anisotropy of the charge-quadrupole and charge-induced dipole interactions favors for a positive point charge, a negative quadrupole moment, and a rodlike molecule with $\alpha_{||} > \alpha_\perp$ a linear configuration over a T-shaped one.[38,59] Indeed, IR spectroscopy and quantum chemical calculations have revealed (nearly) linear intermolecular A−H^+···N−N proton bonds for a variety of AH^+-N_2 dimers (e.g., A = SiO,[49] N_2,[60] C_6H_5O[34]). The situation is similar for the H-bound H_2CCCH^+-N_2 and c-$C_3H_3^+$-N_2 dimers characterized in the present work.

To elucidate the nature of the intermolecular interaction in both $C_3H_3^+$-N_2 dimers in more detail, charge distributions are calculated by using the atoms-in-molecules (AIM) analysis.[45] In c-$C_3H_3^+$ almost the whole positive charge is localized on the three protons ($q_H = 0.27$ e, $q_C = 0.06$ e) leading to the H-bound global minima of c-$C_3H_3^+$-N_2 with a dissociation energy of $D_e = 1227$ cm^{-1}. In H_2CCCH^+ the partial charge on the acetylenic proton ($q_H = 0.32$ e) is significantly larger than that on the CH_2 protons ($q_H = 0.22$ e). Hence, in H_2CCCH^+-N_2 the N_2 ligand prefers binding to the acetylenic C−H proton ($D_e = 1373$ cm^{-1}) over the CH_2 protons ($D_e = 1180$ cm^{-1}). The binding in H-bound c-$C_3H_3^+$-N_2 is slightly weaker than that in H-bound H_2CCCH^+-N_2, consistent with the smaller positive charge on the proton involved in the intermolecular bond. For both dimers, charge transfer from N_2 to the $C_3H_3^+$ ion is calculated to be less than 0.02 e at the equilibrium geometry, implying that the contributions of charge transfer and covalent bonding to the interaction are negligible.

Comparison between c-$C_3H_3^+$-N_2 and $C_6H_6^+$-N_2 reveals the changes in the topology of the intermolecular interaction potential between aromatic hydrocarbon cations and inert ligands (such as N_2) as the size of the aromatic core ion increases. In c-$C_3H_3^+$, a large positive partial charge localized on each single proton causes strong electrostatic and inductive attractions in the H-bound configurations. On the other hand, dispersive forces between the two π electrons of the aromatic c-$C_3H_3^+$ ring and N_2 are small. Hence, the H-bound geometry of c-$C_3H_3^+$-N_2 is more stable than the π-bound structure. In the larger $C_6H_6^+$ ion, the positive charge on each of the six protons is much smaller compared to c-$C_3H_3^+$, whereas the six π electrons give rise to larger dispersion forces. Indeed, IR spectra of $C_6H_6^+$-N_2 are consistent with a π-bound equilibrium structure,[33] which is apparently more stable than the H-bound configuration. Hence, a general rule of thumb for the interaction between aromatic

(59) Olkhov, R. V.; Nizkorodov, S. A.; Dopfer, O. *J. Chem. Phys.* **1997**, *107*, 8229.
(60) Verdes, D.; Linnartz, H.; Maier, J. P.; Botschwina, P.; Oswald, R.; Rosmus, P.; Knowles, P. J. *J. Chem. Phys.* **1999**, *111*, 8400.

hydrocarbon cations and inert neutral ligands may be derived from the comparison between c-$C_3H_3^+$-N_2 and $C_6H_6^+$-N_2: the larger the aromatic ion, the larger the number of polarizable π electrons leading to stronger dispersion forces, and the more delocalized the positive charge leading to weaker electrostatic and induction forces. Thus, π-bound structures gain in stability compared to H-bound structures as the size of the aromatic ion increases.

Experimental and theoretical studies established that the strength of the intermolecular interaction in H-bound AH^+-B dimers is related to the difference in the proton affinities (PA) of the bases A and B.[38,49,61] Considering AH^+-N_2 dimers with $PA(A) \gg PA(N_2) = 494$ kJ/mol,[62] the interaction is stronger for bases with lower PA(A). Complexation with N_2 causes a flattening of the potential for the A−H stretch motion ($\nu_{A-H} = \nu_1$), leading to a red shift in its frequency.[38] The magnitude of the red shift is correlated to the interaction strength and thus to PA(A).[38,49] For example, the PA of H_2CCC is similar to the PA of C_6H_5O (905 vs 873 kJ/mol),[18,63] leading to comparable binding energies and red shifts of the ν_1 vibrations in H-bound H_2CCCH^+-N_2 (5.4%) and $C_6H_5OH^+$-N_2 (4.8%), respectively. In contrast, the $SiOH^+$-N_2 dimer features a much larger ν_1 red shift (14.1%),[49] due to the stronger intermolecular bond arising from the much lower PA of SiO (778 kJ/mol).[62] The intermolecular c-$C_3H_3^+$-N_2 bond is calculated to be weaker than the H_2CCCH^+-N_2 interaction ($D_e = 1227$ vs 1373 cm^{-1}), consistent with the higher PA of c-C_3H_2 compared to H_2CCC (934 vs 905 kJ/mol).[18]

V. Concluding Remarks

Isomeric $C_3H_3^+$-N_2 dimers have been characterized for the first time by spectroscopic and quantum chemical methods. The rovibrational analysis of the IR spectra of $C_3H_3^+$-N_2 dimers reveals the presence of two isomers with C_{2v} symmetry, namely the H-bound H_2CCCH^+-N_2 and c-$C_3H_3^+$-N_2 dimers. Both dimers are global minima on their intermolecular potential energy surfaces and important properties of the intermolecular interaction in these clusters are determined. Perhaps even more significantly, the dimer spectra provide for the first time high-resolution spectroscopic and structural information for the c-$C_3H_3^+$ and H_2CCCH^+ monomer ions in the gas phase. The H_2CCCH^+ ion is shown to have a planar C_{2v} symmetric structure with a linear C−C−C−H$^+$ backbone and an A rotational constant of $A'' \approx 8.500$ cm^{-1}. The planar c-$C_3H_3^+$ ion has almost certainly a structure with D_{3h} symmetry with an A rotational constant of $A'' \approx 1.035$ cm^{-1}. The frequency of the strongly IR active $\nu_4(e')$ mode of c-$C_3H_3^+$ is estimated as 3125 ± 4 cm^{-1}. These results may be useful for the spectroscopic identification of these fundamental hydrocarbon cations in combustion processes or interstellar media.

Acknowledgment. This study is part of project No. 20-63459.00 of the Schweizerischer Nationalfonds. O.D. is supported by the Deutsche Forschungsgemeinschaft via a Heisenberg Stipendium (DO 729/1-1).

JA012004P

(61) Meot-Ner, M. *J. Am. Chem. Soc.* **1984**, *106*, 1257.
(62) Hunter, E. P. L.; Lias, S. G. *J. Phys. Chem. Ref. Data* **1998**, *27*, 413.
(63) Kim, H.; Green, R. J.; Qian, J.; Anderson, S. L. *J. Chem. Phys.* **2000**, *112*, 5717.
(64) Huber, K. P.; Herzberg, G. *Molecular spectra and molecular structure IV. Constants of diatomic molecules*; van Nostrand Reinhold: New York, 1979.